Magneto-mechanical micro-valve for active flow control

Romain Viard, Abdelkrim Talbi, Cécile Ghouila-Houri, Azeddine Kourta, Alain Merlen, Philippe Pernod

Version of Record: https://www.sciencedirect.com/science/article/pii/S0924424720317039
Manuscript_ddf2ec624ebe1068ad28b2dbbb3026a3

Magneto-mechanical micro-valve for active flow control

Romain Viard[(1)], Abdelkrim Talbi [(1,*)], Cécile Ghouila-Houri [(1)], Azeddine Kourta[(2)], Alain Merlen[(1)], Philippe Pernod[(1)]

[(1)] Univ. Lille, CNRS, Centrale Lille, Yncrea Hauts-de-France, Univ. Polytechnique Hauts-de-France, UMR 8520 - IEMN, LIA LICS, F-59000 Lille, France
[(2)] University of Orléans, INSA-CVL, PRISME, EA 4229, 45072, Orléans, France
[(*)] Corresponding author email: abdelkrim.talbi@iemn.fr

Abstract

This paper presents and discusses the development of a normally-off magneto-mechanical airflow microvalve designed for active aerodynamic flow control application. The architecture of the microvalve is composed of a highly flexible mechanical resonator, a miniature coil enabling the magnetic resonator actuation and a packaging with oval shape. The resonator system consists in an elastomer membrane and miniature magnets. The device fabrication process is based on micro-molding, micromachining and rapid prototyping. The pulsed micro-jet delivered by this microvalve can be used at different duty cycles and frequencies going up to 750 Hz. The micro-jet velocity reached 100 m/s for a corresponding airflow rate of 3 L/min. An array of twenty microvalves was implemented on an Ahmed body model and separation flow control experiments were successfully performed. The actuation provided by the micro-jets decreased by 4.3% the drag on the vehicle-like shape.

Keywords

Magneto-mechanical system, Micro-actuator, Pulsed jet, Flow control

1. Introduction

Ecological and economic issues challenge research on transportation: the reduction of CO_2 and NOx emissions is of global concerns and aeronautic and automotive industries need engines with reduced fuel consumption for better performances. A large component of the energy used in ground transportation comes from overcoming aerodynamic drag. At highway speeds, more than 60% of the total resistive force being aerodynamic drag [1]. Hence, one technical way to achieve this goal is to reduce drag on vehicles using flow control. It indeed consists in manipulating a flow field close to a surface in order to produce positive changes in the global flow behaviour, such as the reduction of drag by controlling flow separation. Due to wide variability in the shape of ground vehicle, Ahmed et al (1984) [2] defined a model that has been accepted as the standard of aerodynamic studies on ground vehicles called Ahmed body. This body has a rounded front end and a slanted surface at the trailing edge that produce the major flow structure in the wake [3,4].

Passive or active actuating devices can be used in flow control strategies. Passive devices act permanently and do not need any source of energy to present an effect [5]. Their main issue is that they can bring negative effects when there are not needed. On the contrary, active actuator devices can be turned on or off using an electrical and/or fluidic command. They can be useful when considering closed-loop flow control strategies where sensors detect the moment when flow control is required and send the command to the actuators [6]. The actuators aim then at disturbing the flow by locally modifying its fluidic properties like momentum, velocity or pressure [7]. Actuators in flow control have to meet several requirements. They should be flush mounted to influence near-wall flow phenomena. They also should influence the turbulent flow that is characterized by spatial and temporal scales that are smaller and smaller as the Reynolds number increases. Actuators spatial characteristics should be in the same order of value as these small scales. Also, for practical application, actuator has to have both small size and light weight.

Therefore, MEMS (micro electro mechanical systems) are a technological solution for developing active flow control actuators. First appeared in the late 80s, MEMS now refer to micrometric-millimetric devices, integrating electronics with mechanical components and fabricated using microelectronic techniques. They usually combine sensors, actuators, and processing electronics, providing a high functionality and high-performance integrated microsystems. The main challenge of MEMS actuators for flow control is to provide large forces and displacements for disturbing the turbulent flow field, with highly dense integration in large arrays to fulfill the functional specifications, simultaneously with small sizes, reduced electric and fluidic consumptions, and batch fabrication at reduced unit cost [7].

Several kinds of actuators have therefore been developed for flow control applications and can be classified in different ways. Cattafesta and Sheplak [8] proposed in their review a classification of actuators according to their denomination without

restraining to MEMS devices because of the technological challenges at stake with MEMS. Three main families are listed in [8]: fluidic actuators, plasma actuators and actuators based on the movement of an object of a surface.

In the last family, piezoelectric composite flaps are the most common. Piezoelectric flaps ([9–11]) are usually composed of a cantilever composite beam that can introduce spanwise or streamwise vertical tip as to the local free-stream flow. In 2015, Inaoka et al [12] developed electromagnetic flap actuators used for flow separation control on a airfoil model at low Reynolds number.

The fluidic actuators are the most common in experimental aerodynamics and interest us particularly in this paper. They can be divided into two families: non-zero mass flux actuators and synthetic jets. The first ones need fluid supply and can also be electrically controlled. In this category, one can find continuous jets which only need fluid supply to work. The velocity jet depends on the amount of air flow rate. An electrical signal can be used to close the valve when blowing is not required. The main characteristic of continuous jets lies in the design of the output slot: for a given pressure supply, a small hole or a long thin slot will not give the same kind of jet. However that kind of tehcnology is highly fluid consumming. On the other hand, unsteady jets were developed to generate fluidic vortices. They can be used in flow separation control to add momentum to the flow. Unsteady jets regroup fluidic oscillators and pulsed jet valves. Pulsed jets require a power supply in addition to the fluid supply. The actuator valve alternates between close and open at a chosen frequency to create the vortices. The electrical command (voltage or current) allows changing the actuation frequency in a range determined by the actuator design and materials. Several groups developed MEMS-based pulsed jet actuators working on electrostatic [13], piezoelectric [9] or magnetic actuation as in the LIA LICS in IEMN UMR CNRS 8520 [14–18].

The later produced several generations of pulsed-jet technology, composed of a silicon micro channel, an input orifice with a pressure reservoir on one side and venting to the atmosphere on the other via a sub-millimetric hole. The vibration of the flexible membrane in the micro-channel, controlled by the magnetic actuation, defines the pulsation of the micro-jet. The pulsed-jets obtained reached about 150 m/s of maximum jet velocity for bandwidth as wide as 400 Hz [14], 500 Hz [16] and 1200 Hz [17]. As shown on Figure 1, that kind of performances is of interest for aeronautics. Another kind of non-zero mass flux actuators is fluidic oscillators that do not need any electrical supply to generate vortices but only fluid supply. For example, in sweeping jets, the design makes the fluid oscillating in the valve and generate pulsed jets at a frequency fixed by the design and the airflow. Changing the frequency means changing the airflow and therefore it changes the output velocity. In these devices, each frequency correspond to a given output velocity. Ducloux et al. [19] developed a self-oscillating microvalve based on fluid-structure instability that performed jet with velocities going up to 100 m/s for 1.2 kHz of bandwidth. It is based on the string coupling between a mobile mechanical part (a rigid pad processed on a flexible membrane) and the fluid flow.

Synthetic jets are zero-net mass-flow jets working without fluid supply [20]. They are working by alternating suction and blowing. Gimeno *et al* [18] developed a magnetically actuated MEMS synthetic jet reaching 50 m/s of maximum velocity and 700 Hz of bandwidth. As shown on Figure 1, that kind of performances is of interest for the automobile industry. More recently, Wang *et al* developed MEMS synthetic jets based on piezoelectric PZT thin films [21]. They performed a large bandwidth of 7 kHz but the maximum jet velocity only reached 10 m/s.

In the last 15 years, actuators working on plasma discharge were developed for active flow control. Most of them are dielectric barrier discharge plasma actuators referred as DBD actuators. They are easy to implement in models and present a fast respond. However, they need a high amount of voltage supply, in the range of several kV, and usually generate low velocity jets ([8,22,23]). Caruana et al [24] developed a cavity-based design, with another plasma based working principle to realize a synthetic jet providing velocities up to 100 m/s and a bandwidth of 750 Hz. Nonetheless, the device needed 5 kV to work.

To summarize, works done in the field of actuators for flow control aim at developing devices disturbing the flow. Today, we want maximum jet momentum and minimum volume. Frequency agility is also a requirement because it allows exciting the flow instabilities. Figure 1 presents the main achievements in this research field by comparing the maximum jet velocity and the bandwidth for various fluidic devices. Performances of interest for automobile and aeroautic industries are dispalyed in order to give a concrete goal of the work in this field.

In this paper, we present a normally-off microvalve working as pulsed jet designed for microscale gaseous fluid manipulation and more precisely for aerodynamic flow control application. Flow control on vehicles needs high velocity jets combined with a wide bandwidth of actuation. Meanwhile, the implementation on vehicles require a low volume of occupation and low fabrication costs. In this work, we focused on a low cost miniaturized technology presenting high performances and a wide bandwidth compared to the state of the art of research works on MEMS fluidic actuators. Among microvalves reported in literature, normally-on valves are based on fluidic channel modulation ([15,16]) and require power to close the valves whereas normally-off microvalves, usually based on actuated cantilever design [25], exploit fluid pressure to close it and the actuation is used to open the valve. For this last design, miniaturization induces small displacements leading

to high pressure drop. In this work, we present an alternative principle of operation, using magneto-mechanical interaction coupled with flexible mechanical resonator. This work therefore aimed at at miniaturizing normally-off fluidic valves using an original design and operating principle to minimize and compact the footprint of the device while ensuring high velocity jets and wide actuation frequency bandwidth.

We begin the paper by presenting the microvalve design and working principle and explaining its fabrication process. Then, we describe the characterizations performed on the device that demonstrated its high performances with air medium. Finally, we present an example of scenario for using the microvalve in aerodynamics. We indeed implemented an array of microvalves in an Ahmed body model and used them to control separation at the back of the model.

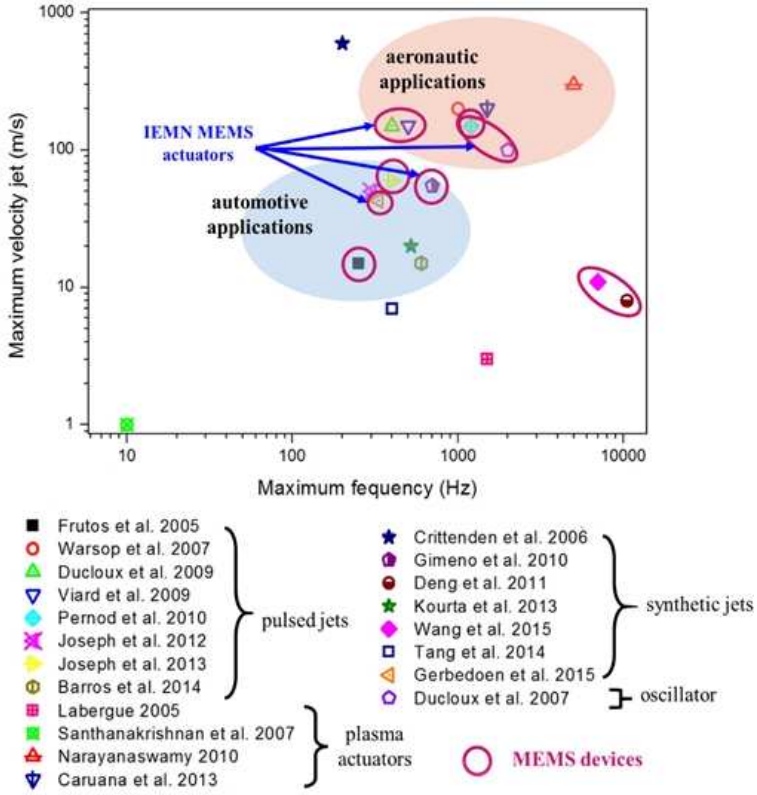

Figure 1: State of the art concerning fluidic actuators for flow control ([13,15–22,24–33])

2. Design and fabrication of the microvalve

The micro-actuator device presented in this paper is characterized by a vertical integration configuration presented in Figure 2, with reduced volume, less than 1 cm3, for easy integration on models or real vehicles. It also enables the manufacturing of a network of microvalve for distributed flow control. As shown on Figure 2, the device is composed of five different parts: an elastomer mechanical resonator, a couple of magnets, a coil, a silicon diaphragm and a package for linear guiding. The airflow goes from the upper part of the structure to the lower packaging where there is the output hole. The set composed of the elastomer resonator and the two magnets forms the flow regulation system.

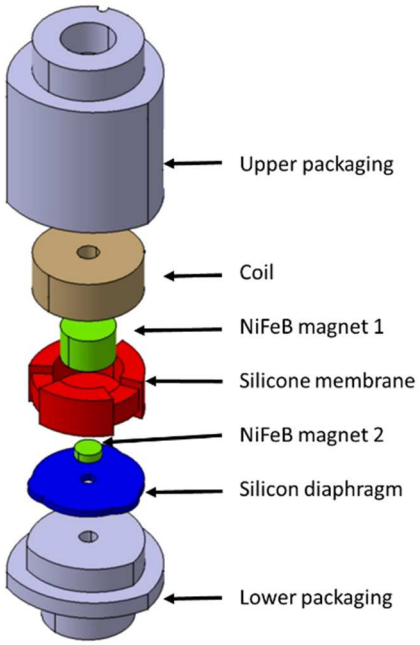

Figure 2: Design of the magneto-mechanical micro-valve

The working principle of the microvalve is displayed in Figure 3.

The actuation is provided by the interaction between the two magnets, placed on both side of the elastomer resonator, and the coil. The two magnets are different in size and repel each other. The biggest magnet is close to the coil and is used to open the microvalve that is normally closed by the fluid. The smallest magnet is close to the silicon diaphragm and ensures that the microvalve is closed without actuation.

The silicon diaphragm guides to the microvalve output jet.

The package is divided into an upper part and a lower part. It is designed in an oval shape (Figure 2) for two reasons. The first one is that the shape of the upper package helps guiding the coil. The second reason is that it enables the realization of three microchannels that perform fluid pressure balance to make the microvalve normally-off.

The design of the microvalve was optimized as regards the spatial dimensions, the performances and the fabrication cost. Magnetic structures highly depends on geometrical parameters and material characteristics (magnetization, permeability, saturation).

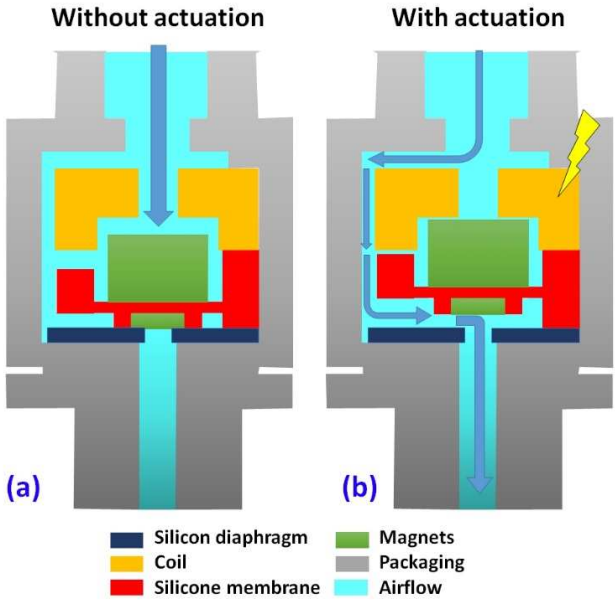

Figure 3: Working principle of the microvalve

Works on the generation of variable magnetization orientation in magnets [34] and on the optimization of the orientation of magnetization in coil / magnet type interactions [35] have been performed in the literature. Given the size of the magnets

wanted for reduced dimensions and cost-relative considerations, we choose not to consider to play on the magnetization to optimize the electromagnetic interaction. The cylindrical magnets with axial magnetization are produced at low cost whereas a magnet with variable magnetization would be more expensive. So we decided to optimize the shape of the coil to maximize the force generated and thus reduce the size of the electromagnet.

The fabrication process of the microvalve was developed to reach low cost manufacturing (Figure 4). Various techniques were employed leading to a hybrid fabrication process, mixing micro-machining, rapid prototyping and micro-moulding. The silicon diaphragm was realized using MEMS micro-machining techniques: photolithography to realize the design and plasma ICP anisotropic etching to produce the part itself. The elastomer resonator was realized using micro-moulding technique. The moulder was manufactured using rapid prototyping and we moulded PDMS (polydimethylsiloxane) elastomer into it. The oval shape packages were also manufactured using rapid prototyping. The two magnets were glued on both sides of the elastomer resonator and the coil was glued on the upper package. Assembly is finally easy enough and this low cost and simple fabrication process appeared to be very reproducible.

A complete set of about 40 microvalves was fabricated. The total volume of each microvalve with packaging is less than 1 cm^3 meaning that the original design and operating principle enable the minimize and compact the footprint of the device. This allows to meet the requirements of automotive and aeronautic industries in terms of aerodynamic flow control.

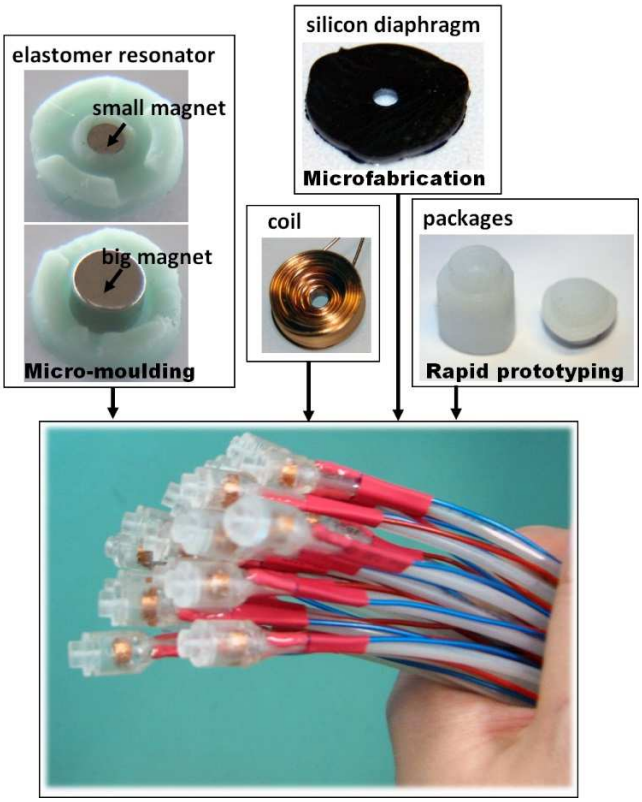

Figure 4: Components of the magneto-mechanical micro-valve

3. Characterizations

Each microvalve was characterized on an experimental bench dedicated to fluidic actuator characterization using air medium. This bench is composed of a Dantec hot-wire probe mounted on a displacement table and an airfluid supply controlled by a flow-meter regulator. The Dantec hot-probe is positioned to measure the flow velocity at the output of the microvalve. With this measurement, we could evaluate the corresponding flow rate. The actuation is provided by a signal generator and a current amplifier. With such an experimental setup, we controlled both the current and the fluid applied to the microvalve.

We first characterized the microvalve in steady blowing mode (Figure 5). In this working mode, we control the flow rate (or velocity jet) by the applied current, for a given airflow pressure supply. The valve is almost closed for 0 A but supplying -0.3 A is enough to perfectly close it for each airflow pressure tested (10, 20 and 30 kPa). By increasing the current, we control the flow rate up to a maximum reached at different current according to the airflow pressure. With 300 kPa of airflow pressure supply and 0.8 A of current supply (equivalent to 1 W of power), we reached more than 100 m/s of output jet velocity. This corresponded of more than 3.5 L/min in flow rate. All microvalves provided the same performances demonstrating the reproducibility of the device.

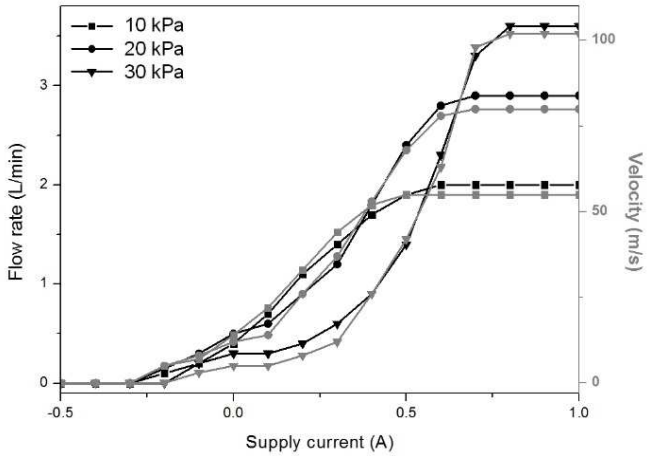

Figure 5: Velocity output (gray) and corresponding flow rate (black) measured for different current and pressure supplies using the microvalve as steady blowing jet

Then, we characterized the microvalve in pulsed jet mode. Instead of applying a DC current to the coil, we applied a square signal, with varying frequency, amplitude and duty cycle. This configurtion helps in saving power as the power is only maximum a fraction of period since the microvalve is normally-off. It is also very interesting in flow control strategies because geneating various eddies allows to disturb the flow at different frequencies, especially the ones for which the flow is particularly sensitive.

Figure 6 presents characterizations performed at 30 Hz, for 20 kPa of pressure supply and for three different duty cycles, 25%, 50% and 75%, with 0.8 A of maximum current intensity. Each result gives the same maximum jet velocity at about 90 m/s. Comparing to Figure 5, pulsed jet mode allowed to reach a higher maximum velocity than steady blowing. The microvalve is optimized for working as a pulsed jet.

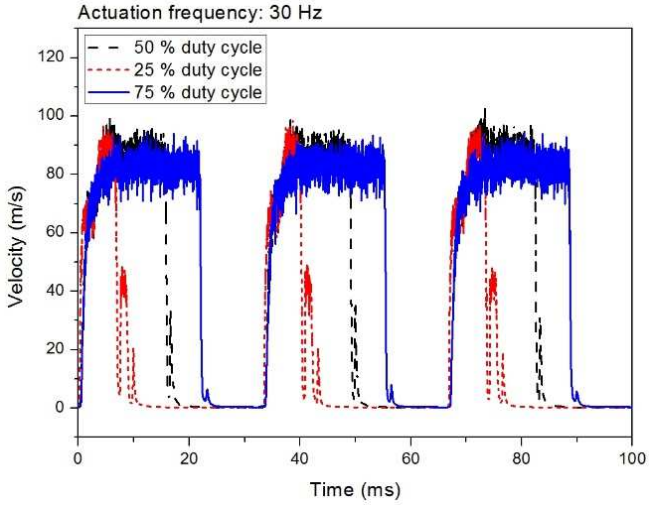

Figure 6: Microvalve response for f = 30 Hz, P = 20 kPa and duty cycle varying between 25 %, 50 % and 75 %

We measured the bandwidth of the microvalve by actuating it with a sine signal, at different frequencies and measuring the amplitude. As shown in Figure 7, the microvalve demonstrated a flat response up to 600 Hz and a cut-off frequency at -3 dB at 700 Hz. Compared to the devices presented in the literature (Figure 1), the microvalve demonstrated performances at the top of the state of the art.

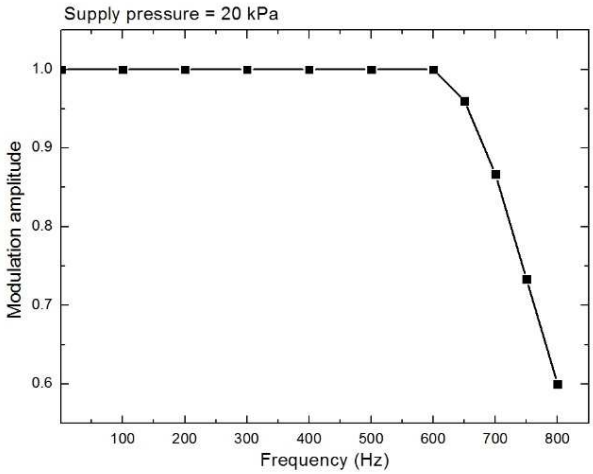

Figure 7: Actuation bandwidth of the micro-valve for a pressure supply of 20 kPa

Afterwards, we could combine different signals for the command. The underlying idea it to disturb the flow at various frequencies simultaneously and to save power. For instance, in Figure 8 (b), we combined a high frequency, 400 Hz, and a low frequency, 30 Hz. In Figure 8 (a), we present the characterization results for an actuation frequency at 400 Hz with 50 % of duty cycle. The velocity reached is more than 100 m/s for 20 kPa of airflow supply and 0.8 A of current. In Figure 8 (b), the command is a burst corresponding to the superposition of a 30 Hz square signal and 400 Hz square signal. The microvalve generates high velocity jets at 400 Hz, all at a frequency of 30 Hz. This mode enables to save power: it generates the 400 Hz vorticies during 16 ms every 33 ms. Moreover, disturbing the flow at both a high frequency and a low frequency can be interesting in flow control strategies. Turbulent flows are indeed characterized by several frequencies: the smaller trubulent structures can present high frequencies but there are also existing low frequencies phenomena, like Von Karman vorticies at 33 Hz. Flow control strategies may be chosen to act on frequency related instabilities. Controlling the microvalve with several caracteristic frequencies of the flow is therefore an added value.

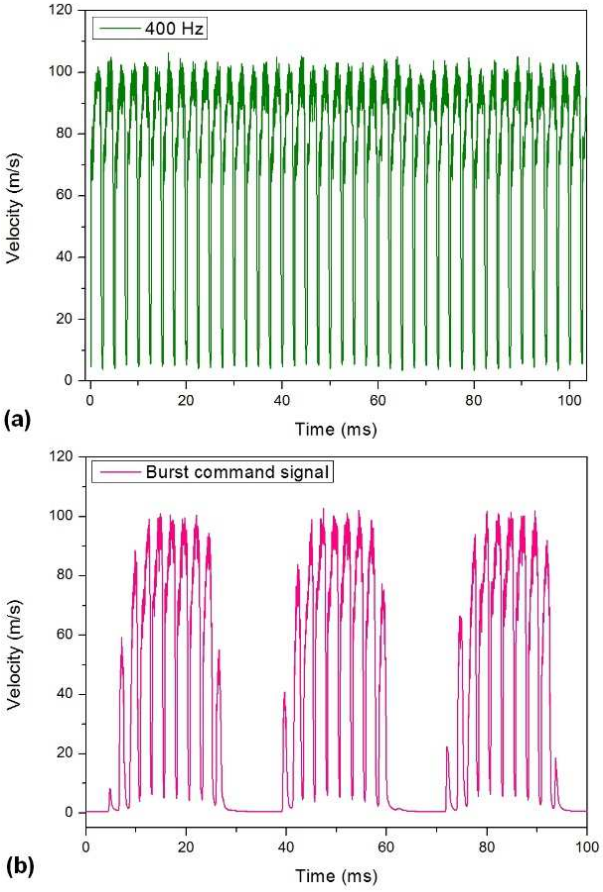

Figure 8: P=20kPa and i=0.8A : (a) Velocity output for 400 Hz of actuation frequency (b) Burst command signal combining 400 Hz and 30 Hz actuation frequencies

4. Active flow control experiments on an Ahmed body model

This part of the paper is devoted to flow control experiments performed using the microvalves on an Ahmed body model (Figure 9 (a)). As has been indicated in the introduction, the Ahmed body [2–5] is widely used in research on automotive industry. It corresponds indeed to the basic shape of a car or a truck. This body shape was widely studied, both in numerical simulations [3,36–39] and experimental tests [4,5,27,28,40–42]. It is basically a cube shape, with designed back and front. Literature shows works on the whole body, or focused on the front or the back. The back is particularly interesting because it is responsible for massive drag in road vehicles due to the contribution of rear body flow structures depending on the rear window angle: separation, wake and longitudinal vortices.

In the experiments, we focused on the back of the Ahmed body at scale 0.75 with a slant angle of 25° (rear window angle). In this case, the separation at the end of the roof intercacts with the two contra-rotating logitudinal vortices issued from both sides of the rear window. This separation reaches the wake. The geometrical characteristics of this model can be found in [3]. To respect the ground clearance, the model is positionned with the help of cicular cylinders. We used a rough band to trip the boundary layer at the roof and to force the turbulent transition and ensure a turbulent boundary layer downsteram along the roof and hence at the rear of the model.

The experiments took place in the S2A wind tunnel. The wind tunnel had an open test section and flow velocities reached up to 40 m/s.

The experimental setup was composed of the Ahmed body model and a Particle Image Velocimetry (PIV) system. The PIV camera could be oriented at different angles to capture several planes. We focused on the side view of the vehicle model when the camera was turned by 90° compared to Figure 9 (a). We implemented an array of 20 microvalves inside the model, with outputs blowing at the top of the rear window. More precisely, in Figure 9 (b) that shows a side view of the Ahmed body model, a yellow arrow points the microvalves outputs.

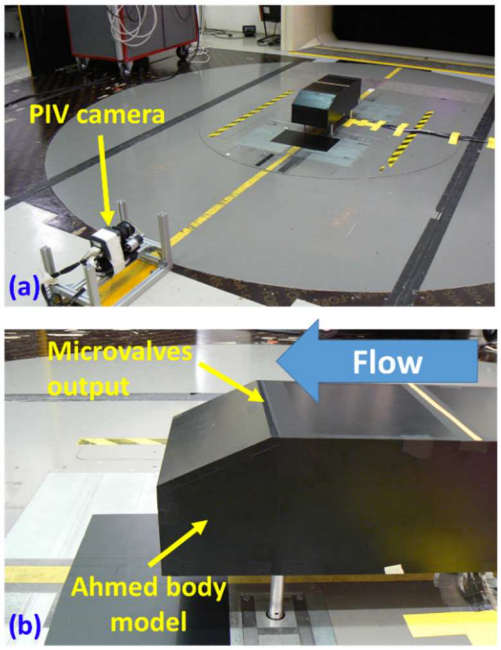

Figure 9: (a) Experimental setup in the CNRT wind tunnel, with the Ahmed body model and the PIV camera (b) Zoom on the Ahmed body model

Figure 10 (a) displays the implementation of the array of 20 microvalves in the top of the rear window of the model. The airflow dispenser and the electronics were embedded inside the Ahmed body model, as seen on Figure 10 (b). We mainly focused to act on the rear window separation.

The experiments were performed with a freestream velocity of $U_\infty = 20\,m/s$. Using the PIV system, we measured the flow velocity fields with and without control around the Ahmed body model. We focused on two planes: rear window separation and the wake at the base. The flow separates at the top edge between the roof and the rear window.

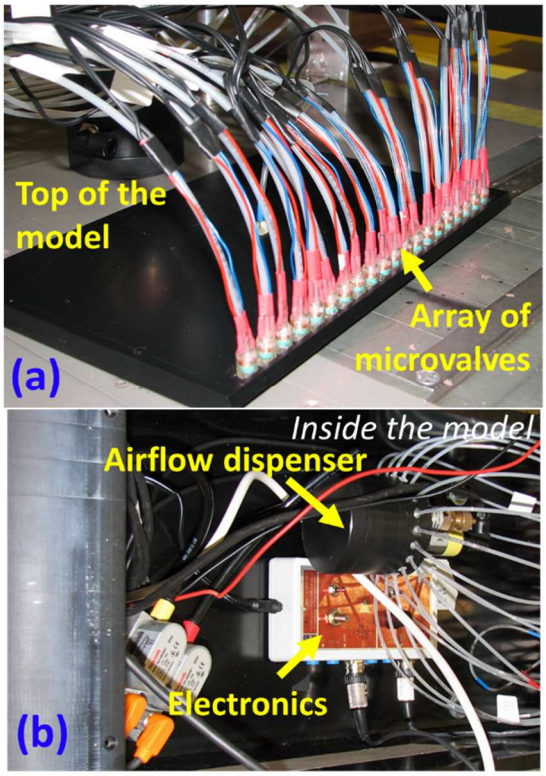

Figure 10: (a) Zoom on the Ahmed body model (b) Implementation of 20 microvalves inside the model

As shown on Figure 11 11, without control, the flow velocity measurements show the separation at the rear window. This separation is characterized by a low velocity area near the wall of the rear window. The flow separates again at the end of the rear window leading to a wake at the rear of the model. In the wake, a massive eddies are observed (recirculation area).

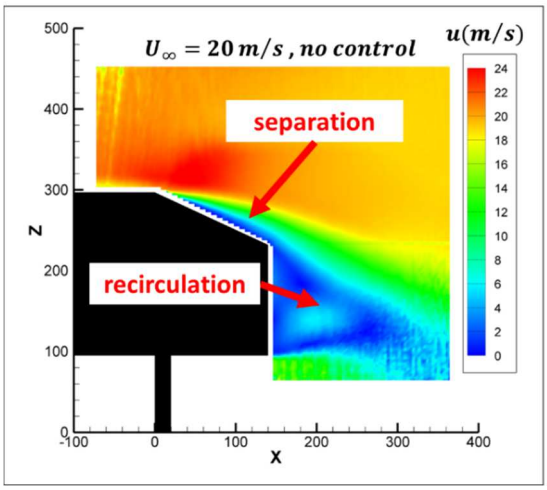

Figure 11: PIV results (side view) for $\boldsymbol{U_\infty = 20\ m/s}$ *without control*

For controlling the flow at the rear of the model, investigations were realized using the valves in continuous jet mode and on pulsed jet mode.

Figure 12 presents the results obtained using the microvalves in continuous jet mode, with an airflow pressure of $P = 20\ kPa$ an a flow rate of about 60 L/min. In Figure 12 (a), one can note the reattachment on the rear window thanks to the jets. Also the separation at the rear of the Ahmed body is not suppressed, however its impact is significantly reduced. Compared to the case without control, the shape of the wake is modified.

In Figure 12 (b), an image treatment was realized to suppress the effect of the wind and visualize correcty the effect of the microvalves array. Even if the jet velocity decreases downstream as we measure away from the microvalve output, the jets

demonstrate an impact overall the rear window and at the back too. So the actuator is able to touch both the rear window separation and the wake at the base.

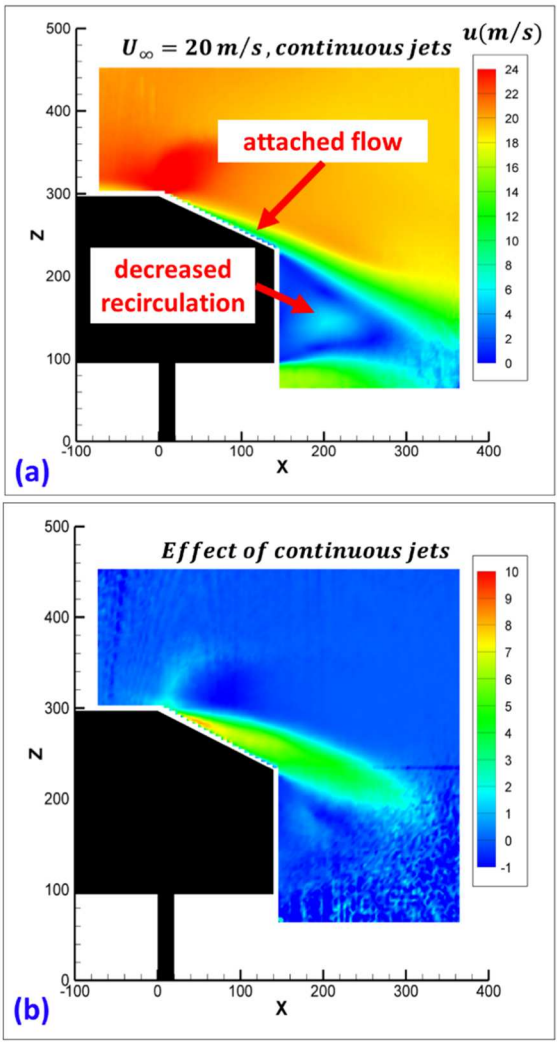

Figure 12: (a) PIV results (side view) for $\boldsymbol{U_\infty = 20\,m/s}$ *with control using continuous jets working mode with* $\boldsymbol{P = 20\,kPa}$*; (b) Visualization of the continuous jets effect*

We then tested the active control on the model using the microvalves in pulsed jet mode, with an airflow pressure of $P = 20\ kPa$ and an actuation frequency of $f = 100\ Hz$, and a duty cycle of 50%. This corresponded to an average flow rate of about 30 L/min for the whole set of microvalves. Compared to continuous mode, we almost save half fluid consumption dut to the fact that the mivrovalves are off half of the time.

The results presented in Figure 13 lead to almost the same conclusions as in Figure 12 (a): pulsed jets succesfully reattached the flow on the rear window and the the shape of the wake at rear is modified but not suppressed. Comparing both PIV images, both control stretagies have the same impacts on the flow as regard the separation on the rear window and the recirculation bubble. However, using the microvalves in pulsed jet mode, we saved both fluid and power. Indeed, as the microvalve is normally-off, the continuous jet mode is highly power consumming.

In terms of aerodynamic performances, the active flow control decreased the drag coefficient by 4.3 %.

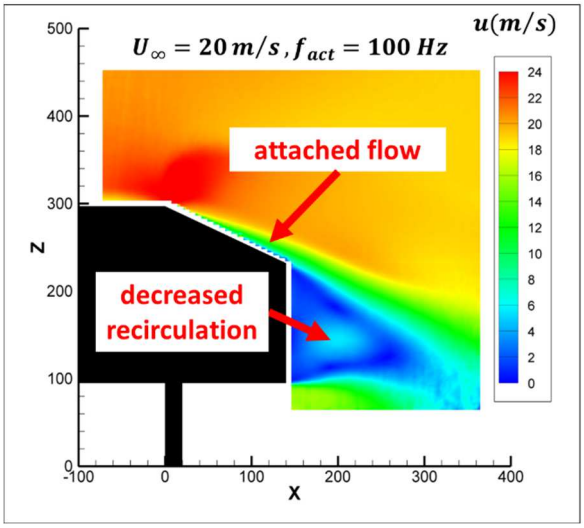

Figure 13. PIV results (side view) for $\boldsymbol{U_\infty = 20\,m/s}$ *with pulsed-jet control, with* $\boldsymbol{P = 20\,kPa}$ *and* $\boldsymbol{f = 100\,Hz}$

5. Conclusion

In this paper, we presented an original magneto-mechanical microvalve, designed for airflow manipulation applications, like active flow control on vehicles. The working principle of the microvalve is based on two points: first the interaction between a mechanical elastomer resonator and a magnetic part composed of two magnets and a coil, and second the original oval-shaped packaging that allows proper fluid guiding and pressure balance. The fabrication used only low-cost techniques, including micromachining, micro-moulding, rapid prototyping. The resulting device is therefore cheap, easy to produce and compatible with mass production.

Characterizations provided demonstration of the microvalve performances, with high flow rates for low power consumption. The wide bandwidth coupled with the high jet velocity place the microvalve device at the state of the art in the domain of aerodynamic flow control.

The demonstration of active flow control on an Ahmed body model was realized using an array of 20 microvalves set on the top of the rear window of the model. Succesfull experiments demonstrated the microvalve device performances for control flow separation on the given configuration of the Ahmed body model. Drag reduction of 4.3% is obtained.

Further work is foreseen for implementing the devices on other configurations and test different flow control strategies such as flow instabilities control.

Acknowledgments

This work was funded by CNRT-R2A. The authors also thank RENATECH, the French national nanofabrication network, FEDER and the the CPER ELSAT 2020 project.

References

[1] W. Hucho, G. Sovran, Aerodynamics of Road Vehicles, Annual Review of Fluid Mechanics. 25 (1993) 485–537. https://doi.org/10.1146/annurev.fl.25.010193.002413.

[2] S.R. Ahmed, G. Ramm, G. Faltin, Some Salient Features Of The Time-Averaged Ground Vehicle Wake, SAE International, Warrendale, PA, 1984. https://doi.org/10.4271/840300.

[3] M. Rouméas, P. Gilliéron, A. Kourta, Separated Flows Around the Rear Window of a Simplified Car Geometry, J. Fluids Eng. 130 (2008). https://doi.org/10.1115/1.2829566.

[4] R. Volpe, P. Devinant, A. Kourta, Experimental characterization of the unsteady natural wake of the full-scale square back Ahmed body: flow bi-stability and spectral analysis, Exp Fluids. 56 (2015) 99. https://doi.org/10.1007/s00348-015-1972-0.

[5] P. Gilliéron, A. Kourta, Aerodynamic drag reduction by vertical splitter plates, Exp Fluids. 48 (2010) 1–16. https://doi.org/10.1007/s00348-009-0705-7.

[6] A. Debien, K.A.F.F. von Krbek, N. Mazellier, T. Duriez, L. Cordier, B.R. Noack, M.W. Abel, A. Kourta, Closed-loop separation control over a sharp edge ramp using genetic programming, Exp Fluids. 57 (2016) 40. https://doi.org/10.1007/s00348-016-2126-8.

[7] P. Pernod, V. Preobrazhensky, A. Merlen, O. Ducloux, A. Talbi, L. Gimeno, N. Tiercelin, MEMS for Flow Control: Technological Facilities and MMMS Alternatives, in: J.F. Morrison, D.M. Birch, P. Lavoie (Eds.), IUTAM Symposium on Flow Control and MEMS, Springer Netherlands, 2008: pp. 15–24. https://doi.org/10.1007/978-1-4020-6858-4_2.

[8] L.N. Cattafesta, M. Sheplak, Actuators for Active Flow Control, Annual Review of Fluid Mechanics. 43 (2011) 247–272. https://doi.org/10.1146/annurev-fluid-122109-160634.

[9] L.N. Cattafesta, S. Garg, D. Shukla, Development of Piezoelectric Actuators for Active Flow Control, AIAA Journal. 39 (2001) 1562–1568. https://doi.org/10.2514/2.1481.

[10] J. Mathew, Q. Song, B.V. Sankar, M. Sheplak, L.N. Cattafesta, Optimized Design of Piezoelectric Flap Actuators for Active Flow Control, AIAA Journal. 44 (2006) 2919–2928. https://doi.org/10.2514/1.19409.

[11] O. Ohanian, C. Hickling, B. Stiltner, E. Karni, K. Kochersberger, T. Probst, P. Gelhausen, A. Blain, Piezoelectric Morphing versus Servo-Actuated MAV Control Surfaces, in: 53rd AIAA/ASME/ASCE/AHS/ASC Structures, Structural Dynamics and Materials Conference, American Institute of Aeronautics and Astronautics, 2012. https://doi.org/10.2514/6.2012-1512.

[12] K. Inaoka, T. Mori, M. Yamaguchi, M. Senda, Feedback flow control of a low-Re airfoil by flap actuators, Journal of Fluids and Structures. 58 (2015) 319–330. https://doi.org/10.1016/j.jfluidstructs.2015.08.011.

[13] J.R. Frutos, D. Vernier, F. Bastien, M. de Labachelerie, Y. Bailly, An electrostatically actuated valve for turbulent boundary layer control, in: IEEE Sensors, 2005., 2005: pp. 7 pp.-. https://doi.org/10.1109/ICSENS.2005.1597642.

[14] O. Ducloux, A. Talbi, Y. Deblock, L. Gimeno, N. Tiercelin, P. Pernod, V. Preobrazhensky, A. Merlen, Magnetically actuated microvalve for active flow control, Journal of Physics: Conference Series. 34 (2006) 631–636. https://doi.org/10.1088/1742-6596/34/1/104.

[15] O. Ducloux, R. Viard, A. Talbi, L. Gimeno, Y. Deblock, P. Pernod, V. Preobrazhensky, A. Merlen, A magnetically actuated, high momentum rate MEMS pulsed microjet for active flow control, J. Micromech. Microeng. 19 (2009) 115031. https://doi.org/10.1088/0960-1317/19/11/115031.

[16] R. Viard, A. Talbi, P. Pernod, V. Preobrazhensky, A. Merlen, Magnetostatic Microvalve for High Momentum Rate Pulsed Jet Generation, Procedia Chemistry. 1 (2009) 421–424. https://doi.org/10.1016/j.proche.2009.07.105.

[17] P. Pernod, V. Preobrazhensky, A. Merlen, O. Ducloux, A. Talbi, L. Gimeno, R. Viard, N. Tiercelin, MEMS magneto-mechanical microvalves (MMMS) for aerodynamic active flow control, Journal of Magnetism and Magnetic Materials. 322 (2010) 1642–1646. https://doi.org/10.1016/j.jmmm.2009.04.086.

[18] L. Gimeno, A. Talbi, R. Viard, A. Merlen, P. Pernod, V. Preobrazhensky, Synthetic jets based on micro magneto mechanical systems for aerodynamic flow control, Journal of Micromechanics and Microengineering. 20 (2010) 075004. https://doi.org/10.1088/0960-1317/20/7/075004.

[19] O. Ducloux, A. Talbi, L. Gimeno, R. Viard, P. Pernod, V. Preobrazhensky, A. Merlen, Self-oscillation mode due to fluid-structure interaction in a micromechanical valve, Applied Physics Letters. 91 (2007) 034101. https://doi.org/10.1063/1.2752530.

[20] A. Kourta, C. Leclerc, Characterization of synthetic jet actuation with application to Ahmed body wake, Sensors and Actuators A: Physical. 192 (2013) 13–26. https://doi.org/10.1016/j.sna.2012.12.008.

[21] S. Wang, B. Ma, J. Deng, H. Qu, J. Luo, Fabrication and characterization of MEMS piezoelectric synthetic jet actuators with bulk-micromachined PZT thick film, Microsyst Technol. 21 (2014) 1053–1059. https://doi.org/10.1007/s00542-014-2278-5.

[22] A. Santhanakrishnan, J.D. Jacob, Flow control with plasma synthetic jet actuators, J. Phys. D: Appl. Phys. 40 (2007) 637. https://doi.org/10.1088/0022-3727/40/3/S02.

[23] V. Boucinha, R. Weber, A. Kourta, Drag reduction of a 3D bluff body using plasma actuators, International Journal of Aerodynamics. 1 (2011).

[24] D. Caruana, F. Rogier, G. Dufour, C. Gleyzes, The plasma synthetic jet actuator, physics, modeling and flow control application on separation, AerospaceLab. (2013) p–1.

[25] C. Warsop, M. Hucker, A.J. Press, P. Dawson, Pulsed Air-jet Actuators for Flow Separation Control, Flow Turbulence Combust. 78 (2007) 255–281. https://doi.org/10.1007/s10494-006-9060-4.

[26] P. Joseph, X. Amandolèse, J.-L. Aider, Drag reduction on the 25° slant angle Ahmed reference body using pulsed jets, Exp Fluids. 52 (2012) 1169–1185. https://doi.org/10.1007/s00348-011-1245-5.

[27] P. Joseph, X. Amandolese, C. Edouard, J.-L. Aider, Flow control using MEMS pulsed micro-jets on the Ahmed body, Exp Fluids. 54 (2013) 1442. https://doi.org/10.1007/s00348-012-1442-x.

[28] D. Barros, T. Ruiz, J. Borée, B. Noack, Control of a three-dimensional blunt body wake using low and high frequency pulsed jets, International Journal of Flow Control. 6 (2014) 61–74. https://doi.org/10.1260/1756-8250.6.1.61.

[29] A. Labergue, Etude de décharges électriques dans l'air pour le développement d'actionneurs plasmas – Application au contrôle de décollements d'écoulements, Thèse, Université de Poitiers, 2005. https://tel.archives-ouvertes.fr/tel-00012120/document (accessed December 3, 2015).

[30] V. Narayanaswamy, L.L. Raja, N.T. Clemens, Characterization of a High-Frequency Pulsed-Plasma Jet Actuator for Supersonic Flow Control, AIAA Journal. 48 (2010) 297–305. https://doi.org/10.2514/1.41352.

[31] T.M. Crittenden, A. Glezer, A high-speed, compressible synthetic jet, Physics of Fluids. 18 (2006) 017107. https://doi.org/10.1063/1.2166451.

[32] J. Deng, W. Yuan, J. Luo, D. Shen, B. Ma, Design and fabrication of a piezoelectric micro synthetic jet actuator, in: Nano/Micro Engineered and Molecular Systems (NEMS), 2011 IEEE International Conference On, IEEE, 2011: pp. 301–304. http://ieeexplore.ieee.org/xpls/abs_all.jsp?arnumber=6017353 (accessed December 3, 2015).

[33] J.-C. Gerbedoen, A. Talbi, R. Viard, V. Preobrazhensky, A. Merlen, P. Pernod, Joint International Laboratory LIA LICS, Elaboration of Compact Synthetic Micro-jets Based on Micro Magneto-mechanical Systems for Aerodynamic Flow Control, Procedia Engineering. 120 (2015) 740–743. https://doi.org/10.1016/j.proeng.2015.08.789.

[34] J. Töpfer, V. Christoph, Multi-pole magnetization of NdFeB sintered magnets and thick films for magnetic micro-actuators, Sensors and Actuators A: Physical. 113 (2004) 257–263. https://doi.org/10.1016/j.sna.2004.04.011.

[35] A. Kruusing, Actuators with permanent magnets having variable in space orientation of magnetization, Sensors and Actuators A: Physical. 101 (2002) 168–174. https://doi.org/10.1016/S0924-4247(02)00154-1.

[36] S. Krajnović, L. Davidson, Flow Around a Simplified Car, Part 1: Large Eddy Simulation, J. Fluids Eng. 127 (2005) 907–918. https://doi.org/10.1115/1.1989371.

[37] S. Krajnović, L. Davidson, Flow Around a Simplified Car, Part 2: Understanding the Flow, J. Fluids Eng. 127 (2005) 919–928. https://doi.org/10.1115/1.1989372.

[38] M. Rouméas, P. Gilliéron, A. Kourta, Drag reduction by flow separation control on a car after body, International Journal for Numerical Methods in Fluids. 60 (2009) 1222–1240. https://doi.org/10.1002/fld.1930.

[39] M. Rouméas, P. Gilliéron, A. Kourta, Analysis and control of the near-wake flow over a square-back geometry, Computers & Fluids. 38 (2009) 60–70. https://doi.org/10.1016/j.compfluid.2008.01.009.

[40] E. Bideaux, P. Bobiller, P. Gillièron, P. Gilotte, M. El Hajem, J. Champagne, A. Kourta, Drag reduction by pulsed jets on strongly unstructured wake: towards the square back control, Int. J. Aerodynamics. 1 (2011) 282–298.

[41] S. Aubrun, J. McNally, F. Alvi, A. Kourta, Separation flow control on a generic ground vehicle using steady microjet arrays, Exp Fluids. 51 (2011) 1177–1187. https://doi.org/10.1007/s00348-011-1132-0.

[42] J. McNally, N. Mazellier, F. Alvi, A. Kourta, Control of salient flow features in the wake of a 25° Ahmed model using microjets, Exp Fluids. 60 (2018) 7. https://doi.org/10.1007/s00348-018-2645-6.

Magneto-Machenical Normally-Off Microvalve